

PIMS Modulates Immune Tolerance by Negatively Regulating *Drosophila* Innate Immune Signaling

Nouara Lhocine,^{1,7} Paulo S. Ribeiro,^{2,6,7} Nicolas Buchon,³ Alexander Wepf,^{4,5} Rebecca Wilson,² Tencho Tenev,² Bruno Lemaître,^{1,3} Matthias Gstaiger,^{4,5,8} Pascal Meier,^{2,8,*} and François Leulier^{1,8,*}

¹CNRS, Centre de Génétique Moléculaire, UPR2167, Gif-sur-Yvette, F-91198, France

²Breakthrough Toby Robins Breast Cancer Research Centre, Institute of Cancer Research, London SW3 6JB, England, UK

³EPFL, Global Health Institute, Lausanne, CH-1015, Switzerland

⁴ETH, Institute for Molecular Systems Biology, Wolfgang-Pauli-Street 16, CH-8093 Zurich, Switzerland

⁵Competence Center for Systems Physiology and Metabolic Diseases, ETH Zurich, 8093 Zurich, Switzerland

⁶Programa Gulbenkian de Doutorado em Biomedicina, Instituto Gulbenkian de Ciência, Apartado 14, Oeiras 2781-901, Portugal

⁷These authors contributed equally to this work

⁸These authors contributed equally to this work

*Correspondence: pmeier@icr.ac.uk (P.M.), leulier@cgm.cnrs-gif.fr (F.L.)

DOI 10.1016/j.chom.2008.07.004

SUMMARY

Metazoans tolerate commensal-gut microbiota by suppressing immune activation while maintaining the ability to launch rapid and balanced immune reactions to pathogenic bacteria. Little is known about the mechanisms underlying the establishment of this threshold. We report that a recently identified *Drosophila* immune regulator, which we call PGRP-LC-interacting inhibitor of Imd signaling (PIMS), is required to suppress the Imd innate immune signaling pathway in response to commensal bacteria. *pims* expression is *Imd* (immune deficiency) dependent, and its basal expression relies on the presence of commensal flora. In the absence of PIMS, resident bacteria trigger constitutive expression of antimicrobial peptide genes (AMPs). Moreover, *pims* mutants hyperactivate AMPs upon infection with Gram-negative bacteria. PIMS interacts with the peptidoglycan recognition protein (PGRP-LC), causing its depletion from the plasma membrane and shutdown of Imd signaling. Therefore, PIMS is required to establish immune tolerance to commensal bacteria and to maintain a balanced Imd response following exposure to bacterial infections.

INTRODUCTION

Metazoans live in close contact with a multitude of microbes with which they establish complex reciprocal interactions. Some of these relationships result in commensalism, where one partner benefits and the other remains unharmed, while others can range from colonization to infectious disease (Casadevall and Pirofski, 2000). Most interactions between host and micro-organisms do not result in disease and, instead, are essential to many aspects of normal host physiology, contributing to metabolic activities

and immune homeostasis (Backhed et al., 2005). Nonpathological host-microbe interactions depend on intrinsic properties of the microbe and the host's ability to control its indigenous microbiota. Together, this forms a homeostatic relationship, which when uncoupled, can result in pathological outcomes (Macdonald and Monteleone, 2005). For a host to tolerate a certain amount of resident bacteria, it is critical that the activation threshold of the immune response is under tight control. Moreover, upon infection, the strength and timing of the immune response must be adjusted so that the homeostatic host-microbe interaction can be re-established (Artis, 2008). The immune response of the gut is complex since it needs to respond strongly to ingested pathogenic bacteria, while tolerating food antigens and commensal microbiota (Macdonald and Monteleone, 2005). This ability of the gut is commonly referred to as immune tolerance (Müller et al., 2005). Although commensalism exists in all metazoans, the underlying molecular mechanism of immune tolerance remains largely unknown.

Like vertebrates, *Drosophila* protects itself from bacterial and fungal infections through physical barriers, local immune reactions, and systemic responses (Lemaître and Hoffmann, 2007). Following exposure to infectious micro-organisms, the gut and tracheal epithelia, which are both exposed to the external milieu and microbiota, secrete antimicrobial peptides (AMPs) and reactive oxygen species (ROS) (Ferrandon et al., 1998; Ha et al., 2005a; Önfelt Tingvall et al., 2001; Tzou et al., 2000). In addition, circulating and tissue-restricted phagocytic cells engulf foreign intruders and thereby complement the response of the gut or tracheal epithelia (Stuart and Ezekowitz, 2008). The fat body, the functional equivalent of the mammalian liver, ultimately triggers the systemic response producing large amounts of humoral immune effectors that include AMPs (Ferrandon et al., 2007).

The *Drosophila* gut serves as a useful model system to study both immune tolerance and local immune reactions to bacterial infections. Ingested noncommensal bacteria trigger the production of ROS and AMPs in the gut (Ha et al., 2005a; Liehl et al., 2006; Nehme et al., 2007; Ryu et al., 2006). Commensal bacteria, however, do not elicit such a response. Although little is known

on how immune tolerance is established, recent evidence indicates that both the immune-regulated catalase (IRC) and the transcriptional repressor Caudal are indispensable. While IRC buffers the redox status of the gut (Ha et al., 2005b), the homeobox protein Caudal suppresses NF- κ B-mediated AMP expression in the posterior part of the midgut following exposure to commensals (Ryu et al., 2008). Disruption of Caudal causes severe defects in the mutualistic interaction between gut and commensal bacteria.

Systemic infection by Gram-negative bacteria triggers activation of the *Drosophila* immune deficiency (Imd)-signaling pathway that culminates in activation of Relish, a member of the Rel/NF- κ B family of transcription factors. Relish, in turn, activates a transcriptional program dedicated to kill infective microbes (Ferrandon et al., 2007). Exposure to fungi and Gram-positive bacteria, on the other hand, activate the Toll pathway and the NF- κ B family members Dorsal and Dif, which induce expression of peptides that target fungi and Gram-positive bacteria (Ferrandon et al., 2007).

The presence of commensal bacteria, like exposure to oral or systemic Gram-negative bacterial infection, activates the Imd pathway via DAP-type peptidoglycan (DAP-PGN), a major component of the Gram-negative bacterial cell wall (Leulier et al., 2003; Ryu et al., 2008; Zaidman-Rémy et al., 2006). DAP-PGN binds to the transmembrane receptor peptidoglycan recognition protein (PGRP)-LC, both in the gut and fat body. Upon binding, PGRP-LC and PGRP-LE—another member of the PGRP family—stimulate the recruitment of a signaling complex that ultimately activates Relish (Choe et al., 2002; Gottar et al., 2002; Takehana et al., 2004). Activation of Relish requires the coordinated action of the *Drosophila* IKK complex (Kenny/Ird5), which phosphorylates Relish, and the initiator caspase Dredd, which removes its C-terminal inhibitory domain (Silverman et al., 2000; Stöven et al., 2003). This enables translocation of Relish to the nucleus and expression of several target genes that include AMPs (De Gregorio et al., 2002).

Since spontaneous activation or prolonged immune response is detrimental to the host (Bischoff et al., 2006; Kim et al., 2007; Maillet et al., 2008; Ryu et al., 2008), it is vital that Imd signaling is subject to negative regulation. A few negative regulators of Imd signaling have been identified. PGRP-LF prevents constitutive signaling of Imd and JNK pathways by antagonizing PGRP-LC activation (Maillet et al., 2008), while Caspar and the defense repressor 1 (Dnr1) block Dredd-mediated induction of Relish (Foley and O'Farrell, 2004; Kim et al., 2006). SCF^{Slimb}, an E3 ubiquitin-ligase complex, suppresses Imd signaling by targeting Relish for degradation (Khush et al., 2002). Moreover, a repressosome complex—containing Dsp1, dAP-1, and STAT92E—removes Relish from the promoters of immune effector genes and recruits histone deacetylases to block transcription (Kim et al., 2007). The immune modulators PGRP-SC1/2 and PGRP-LB, which carry peptidoglycan amidase activity, antagonize Imd signaling by reducing the amount of available DAP-PGN (Bischoff et al., 2006; Zaidman-Rémy et al., 2006). Consequently, PGRP-SC1/2 and PGRP-LB modulate the intensity of the immune response. Intriguingly, expression of PGRP-LB is under the control of the Imd pathway, providing negative-feedback control to adjust the immune response upon infection (Zaidman-Rémy et al., 2006). In addition, PGRP-SC1/2 and PGRP-LB also play impor-

tant roles in establishing immune tolerance (Bischoff et al., 2006; Zaidman-Rémy et al., 2006).

While most positive regulators of the Imd pathway have been identified by genome-wide RNAi and classical mutagenesis screens, little is known how this pathway is negatively regulated to allow immune tolerance and achieve balanced immune responses. Here we report that a recently identified *Drosophila* immune regulator (Kleino et al., 2008), which we call PGRP-LC-interacting inhibitor of Imd signaling (PIMS), is required to suppress Imd signaling in response to commensal bacteria and following oral and systemic infection. We demonstrate that *pims* expression is Imd dependent and that its basal expression relies on the presence of commensal flora. In the absence of PIMS, resident bacteria trigger strong local expression of antimicrobial peptide genes (AMPs), while ingested bacteria trigger robust systemic expression of AMPs. Moreover, *pims* mutant animals hyperactivate AMPs upon systemic infection with Gram-negative bacteria. Furthermore, we show that PIMS interacts with PGRP-LC and causes a profound change of its subcellular localization leading to depletion of PGRP-LC from the plasma membrane and shutdown of Imd-signaling in a negative-feedback loop. Together, our data are consistent with a model whereby a balanced immune response is achieved by PIMS-mediated regulation of PGRP-LC receptor availability.

RESULTS

Infection Induces *pims* Expression in a Relish-Dependent Manner

Large-scale microarray analysis has identified genes that are induced following exposure to Gram-negative bacteria in *Drosophila*. Among others, *CG15678* was identified as being strongly induced in an Imd pathway-dependent manner (De Gregorio et al., 2002; Kallio et al., 2005). Moreover, RNAi-mediated down-regulation of *CG15678* in tissue-culture cells leads to constitutive, low-level expression of some transcriptional target genes of the Imd pathway (De Gregorio et al., 2002; Kallio et al., 2005), suggesting that *CG15678* may function as a negative regulator of Imd signaling. To gain insights into the physiological role of *CG15678*, we first analyzed the kinetics of *pims* induction in different models of microbial infection. Infection by septic injury resulted in a marked (13-fold) induction of *pims* expression within 1 hr of exposure to the Gram-negative bacteria *Escherichia coli* (*E. coli*) (Figure 1A). Importantly, *pims* induction was strictly Relish dependent since *Relish*^{E20} mutant flies failed to activate *pims* expression. Relish-mediated induction of *pims* was also observed after oral infection (Figure 1B). In this system, animals are naturally infected via the digestive tract through exposure to food contaminated with the Gram-negative bacteria *Erwinia carotovora carotovora 15* (*Ecc15*) (Basset et al., 2000). Inspection of the putative regulatory region of *pims* revealed the presence of four putative κ B DNA-binding sites within 1.2 kb of its transcriptional start site (Figure 1C). The κ B site at position -506 bp perfectly matches the DNA-binding consensus motif of Relish (Busse et al., 2007).

Basal *pims* Expression in the Gut Requires Exposure to Commensal Bacteria

The gut epithelia of conventionally reared *Drosophila* is in close proximity with a large number of commensal bacteria (about

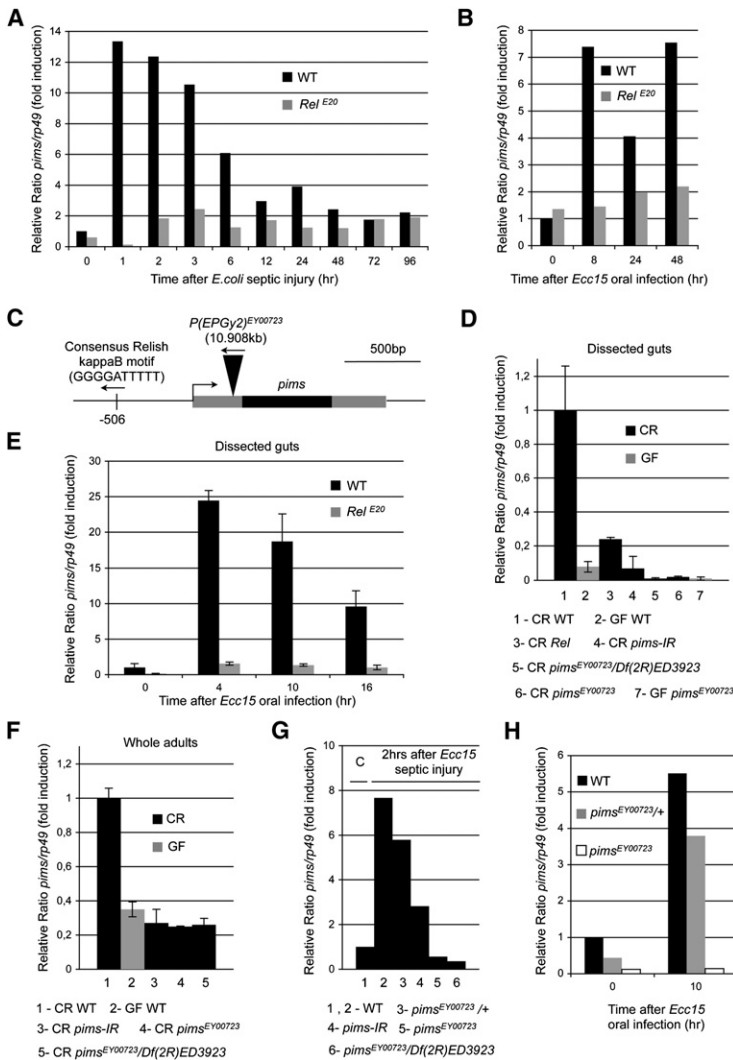


Figure 1. *pims* Expression Is Dependent on Relish and Commensal Bacteria

(A and B) *pims* expression upon infection in whole flies. Quantitative RT-qPCR analysis of *pims* induction in *Canton^S* and *Relish^{E20}* flies upon *E. coli* septic injury (A) and *Ecc15* oral infection (B) is shown.

(C) Schematic representation of the *pims* locus.

(D and E) *Relish*-dependent expression of *pims* in the gut is driven by resident and infectious bacteria. In (D), basal *pims* expression in guts of conventionally reared *Canton^S* (*CR^{WT}*), *Relish^{E20}* (*CR^{Rel}*), *Da-GAL4 > pims-IR* (*CR^{pims-IR}*), *pims^{EY00723}/Df(2R)ED3923* (*CR^{pimsEY00723/Df(2R)ED3923}*), *pims^{EY00723}* (*CR^{pimsEY00723}*), germ-free *Canton^S* (*GF^{WT}*), and *pims^{EY00723}* (*GF^{pimsEY00723}*) flies is shown. In (E), *pims* expression in dissected guts of *Canton^S* and *Relish^{E20}* flies upon oral infection by *Ecc15* is shown.

(F) *pims* expression in *CR^{WT}*, *CR^{pims-IR}*, *CR^{pimsEY00723}*, *CR^{pimsEY00723/Df(2R)ED3923}*, and *GF^{WT}* flies. Relative *pims* expression in the indicated WT and mutant flies following *Ecc15* septic injury (G) and *Ecc15* oral infection (H) is shown. *rp49* was used as the experimental expression standard. Graphs represent the mean \pm SD of relative *pims*/*rp49* ratios detected in three biological repetitions of a pool of 20 dissected guts (D–E) and flies (F).

sals also trigger gut-specific expression of *PGRP-SC1* and *PGRP-LB*, two previously characterized negative regulators of the Imd pathway (Ryu et al., 2008) (N.B. and B.L., unpublished data). The observation that *PGRP-SC1*, *PGRP-LB*, and *pims*, (but not AMP genes) are expressed in guts harboring commensals suggests that *pims*—like *PGRP-SC1* and *PGRP-LB*—functions as a negative regulator of Imd signaling. Moreover, in response to oral infection by *Ecc15*, *pims* expression in the gut increased even further and was induced 24-fold above basal levels (Figure 1E), a feature also seen for *PGRP-SC1* and *PGRP-LB* (N.B. and B.L., unpublished data). Like in nonchallenged conditions, *Relish^{E20}* mutant flies did not induce *pims* expression following oral infection (Figure 1E). Therefore, these results indicate that *pims* expression in the gut requires the presence of intestinal bacteria.

Our data are consistent with a model in which *pims* participates in a negative-feedback loop that regulates the activity of the Imd pathway. To test this, we characterized a mutant *pims* allele (*pims^{EY00723}*) and used RNAi-mediated knockdown in vivo (*pims-IR*). *pims^{EY00723}* mutant flies carry a transposon-inserted 62 bp upstream of the translational start site of *pims* (Figure 1C). *pims^{EY00723}* homozygous mutant animals are viable and fertile but display a marked reduction of their life span (N.L. and F.L., unpublished data). Gut-specific expression of *pims* was completely abolished in conventionally reared homozygous *pims^{EY00723}* and hemizygous *pims^{EY00723/Df(2R)ED3923}* mutants. *pims* expression in the gut of these animals was similar to the one of WT flies grown under axenic conditions (Figure 1D). Moreover, daughterless GAL4-driven *pims* RNAi (*pims-IR*) resulted in significant reduction of *pims* expression in the gut (Figure 1D). Basal expression of *pims* in whole flies raised under conventional conditions was markedly reduced in *pims-IR*, *pims^{EY00723}*, and *pims^{EY00723/Df(2R)ED3923}* mutants. Basal expression of *pims* was also similar to *pims* levels of *GF^{WT}* flies

10^6 in old flies) that are well tolerated and, under normal condition, do not elicit an innate immune response (Ren et al., 2007; Ryu et al., 2008). To examine whether *pims* expression is influenced by commensal bacteria, we compared conventionally reared wild-type flies (*CR^{WT}*) with *Relish^{E20}* mutant flies (*CR^{Rel}*) and flies that were cultured under germ-free (*GF^{WT}*) conditions (see Figure S1 available online). In *CR^{WT}* animals, *pims* expression was readily detected in adult guts (Figure 1D), while it was essentially absent in other parts of the body (Chintapalli et al., 2007). Adult midguts showed highest levels of *pims* expression that were at least 10-fold above the levels of other tissues. Moreover, *pims* expression was also significantly elevated in the crop and hindgut (Chintapalli et al., 2007). Gut-specific expression of *pims* was *Relish* dependent since guts of *CR^{Rel}* animals showed only background levels of *pims* (Figure 1D). Importantly, like *CR^{Rel}* animals, guts from *GF^{WT}* animals—which were reared under axenic conditions—displayed similar low basal levels of *pims* expression (Figure 1D). The observation that *pims* levels are low in *CR^{Rel}* and *GF^{WT}* animals in comparison to guts from *CR^{WT}* animals strongly suggests that *pims* expression in the gut is driven by the exposure to commensal microbiota. Similarly, commensal

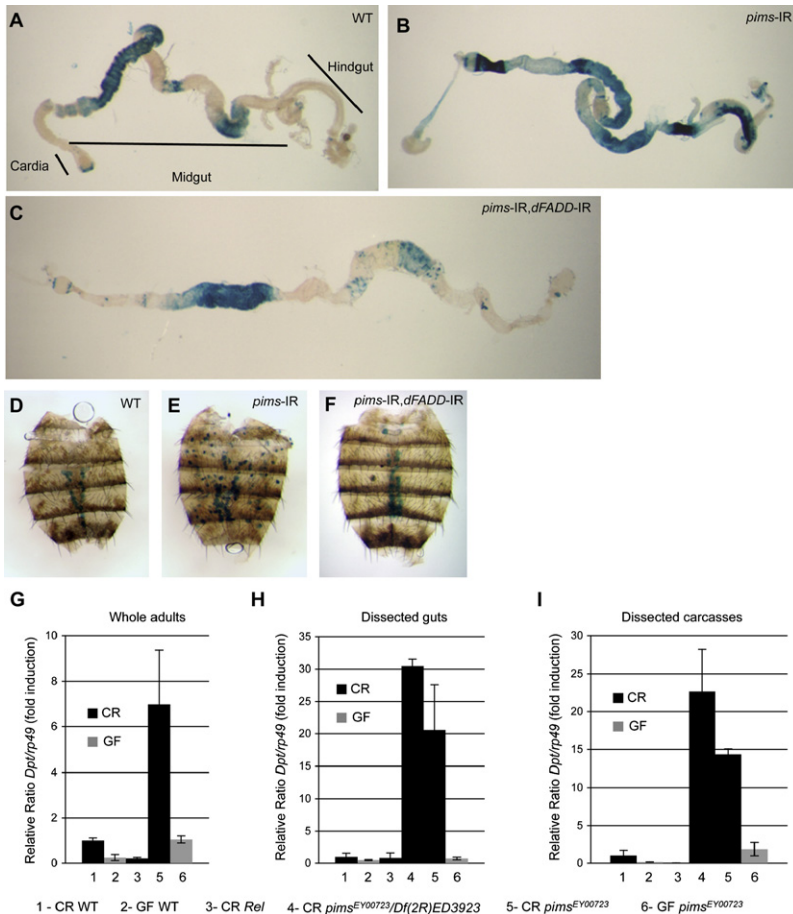


(Figure 1F). Thus, in comparison to CR^{WT} animals, *pims* levels were significantly lower in CR^{*pims^{EY00723}*}, CR^{*pims^{EY00723}/Df(2R)ED3923*}, and GF^{WT} flies, suggesting that *pims^{EY00723}* is a null mutation. Furthermore, this observation is consistent with the notion that basal *pims* expression is driven by exposure to commensal microbiota.

Homozygous and hemizygous *pims* mutants completely failed to induce *pims* expression following exposure to Gram-negative bacteria via septic injury or oral infection (Figures 1G, 1H, and data not shown). Moreover, *pims-IR* flies and heterozygous *pims^{EY00723}/+* mutants also showed a significantly reduced induction of *pims* (Figures 1G, 1H, and data not shown). Therefore, these results indicate that *pims^{EY00723}* behaves like a null mutation following septic and oral infection, while *pims^{EY00723}/+* and *pims-IR* generate hypomorphic effects.

PIMS Blocks AMPs Production in Response to Commensal Microbiota

To investigate the role of *pims* in innate immunity, we analyzed the basal expression levels of *Diptericin* (*Dpt*), an AMP gene controlled by the Imd pathway. *Dpt* expression was evaluated using a *Dpt-LacZ* reporter transgene, which accurately recapitulates the expression pattern of endogenous *Dpt* expression (Meister et al., 1994). In the majority of untreated WT flies (82%, n = 22), β-galactosidase activity was restricted to two segments of the middle midgut (Figure 2A), and no significant reporter gene expression was observed in other parts of the cardia, midgut,

Figure 2. PIMS Prevents AMP Production in the Presence of Commensal Microbiota

(A–C) Ectopic activation of *Diptericin-LacZ* (*Dpt-LacZ*) in *pims-IR* adult guts. In (A), representative X-gal staining of a *Dpt-LacZ;Da-GAL4/+* gut (82%, n = 22) is shown. The three main regions of the adult gut (cardia, midgut, and hindgut) are shown. Constitutive LacZ activity of the middle midgut is likely due to endogenous β-galactosidase activity. X-gal staining of guts from (B) *Dpt-LacZ; Da-GAL4 > pims-IR* flies (88%, n = 69) and (C) *Dpt-LacZ;Da-GAL4 > pims-IR,dFADD-IR* flies (100%, n = 24) is shown. Anterior is to the left, and posterior is to the right.

(D–F) Ectopic activation of *Dpt-LacZ* in *pims-IR* adult carcasses. X-gal staining of a (D) *Dpt-LacZ; Da-GAL4/+* carcass (91%, n = 23), (E) *Dpt-LacZ; Da-GAL4 > pims-IR* carcass (46%, n = 69), and a (F) *Dpt-LacZ; Da-GAL4 > pims-IR,dFADD-IR* carcass (100%, n = 26) is shown.

(G–I) Deregulation of *Dpt* expression in *pims* mutant. In (G), quantitative RT-qPCR analysis of *Dpt* expression in conventionally reared *Canton^S* (CR^{WT}), *Relish^{E20}* (CR^{Rel}), *pims^{EY00723}/Df(2R)ED3923* (CR^{*pims^{EY00723}/Df(2R)ED3923*}), *pims^{EY00723}* (CR^{*pims^{EY00723}*}), germ-free *Canton^S* (GF^{WT}), and *pims^{EY00723}* (GF^{*pims^{EY00723}*}) flies (G), guts (H), and carcasses (I) is shown. *rp49* was used as the experimental expression standard. Graphs represent the mean ± SD of relative *Dpt/rp49* ratios detected in three biological repetitions of a pool of 20 flies (G), dissected guts (H), or carcasses (I).

and hindgut. However, in rare cases (18%, n = 22), weak LacZ staining was also observed in the anterior portion of the midgut (data not shown). Interestingly, RNAi-mediated knockdown of *pims* resulted in ectopic expression of *Dpt-LacZ* throughout the anterior and posterior midgut as well as in the hindgut (88%, n = 69) (Figure 2B)—a pattern that is highly similar to the one seen in *Ecc15*-infected guts (N.B. and B.L., unpublished data). Ectopic induction of *Dpt-LacZ* expression was dependent on Imd signaling since it was lost in *pims-IR* flies that were simultaneously depleted of the adaptor protein *dFADD*, which is essential for Imd signaling (Figure 2C) (Leulier et al., 2002). Similarly, ectopic *Dpt-LacZ* expression was also observed in the carcass of *pims-IR* flies. Under these conditions, 46% (n = 69) of *pims-IR* flies displayed ectopic *Dpt-LacZ* activity in the fat body, which is attached to the carcass (Figure 2E), whereas 91% of WT flies (n = 23) showed no expression (Figure 2D). Like in the gut, concomitant RNAi of *pims* and *dFADD* abolished ectopic *Dpt-LacZ* expression (Figure 2F). The notion that knockdown of *dFADD* suppresses the *pims* RNAi phenotype indicates that *pims* functions genetically upstream of *dFADD*.

Next, we examined the expression levels of endogenous *Dpt* in *pims* mutant animals. Homozygous *pims^{EY00723}* mutants showed a 7-fold induction of basal *Dpt* expression when compared to WT controls (Figure 2G). This phenotype was much more striking in isolated guts of *pims^{EY00723}* and *pims^{EY00723}/Df(2R)ED3923* mutants,

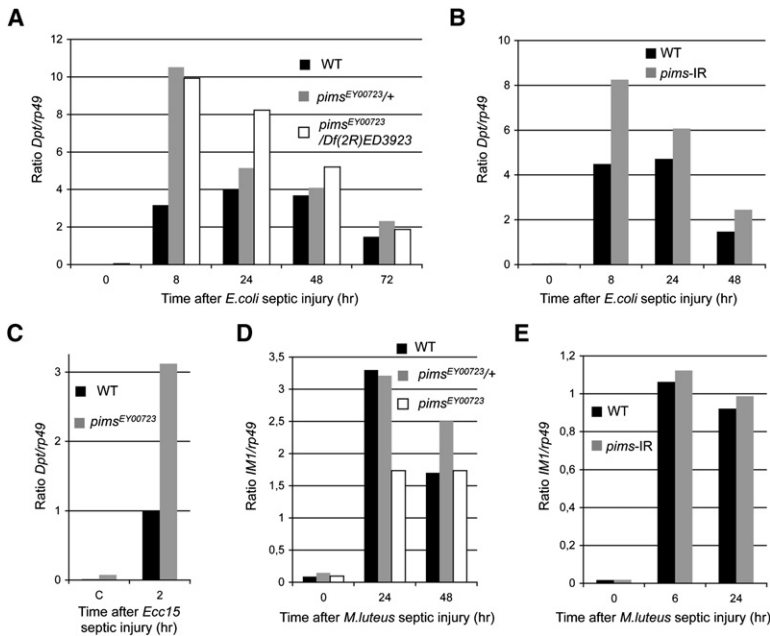


Figure 3. Loss of *pims* Results in Hyperactivation of the Imd Response Following Systemic Infection

(A–C) Quantitative RT-qPCR analysis of *Dpt* induction after Gram-negative bacteria septic injury. *Dpt* expression upon *E. coli* septic injury of (A) Canton^S, *pims^{EY00723/+}* and *pims^{EY00723}/Df(2R)ED3923* flies, (B) *Da-GAL4/+* and *Da-GAL4 > pims-IR* flies, and (C) Canton^S and *pims^{EY00723}* flies is shown.

(D–E) Quantitative RT-qPCR analysis of *IM1* induction after *M. luteus* septic injury. *IM1* expression in (D) Canton^S, *pims^{EY00723/+}* and *pims^{EY00723}* flies, and (E) *Da-GAL4 > pims-IR* flies is shown. *tp49* was used as the experimental expression standard.

which had dramatically elevated levels of *Dpt* expression (20- to 30-fold induction, respectively). Similar results were obtained from isolated carcasses (15- to 22-fold induction, respectively) (Figures 2H and 2I). Although *pims* mutant flies have elevated basal levels of *Dpt*, this level merely represents 1% of the induced levels that is achieved after 8 hr following a systemic bacterial infection.

The elevated basal levels of *Dpt* expression in *pims* mutants were dependent on the presence of commensal microbiota, since this phenotype was rescued when these flies were raised under sterile conditions (Figures 2G–2I). While *pims* mutant flies had high basal levels of *Dpt* expression, *pims^{EY00723}* animals that were raised under axenic conditions displayed low basal levels of *Dpt* expression, which were comparable to the ones of CR^{WT} flies (Figures 2G–2I). Under these conditions, CR^{Rel} and GF^{WT} animals displayed extremely low basal levels of *Dpt* expression in their guts and carcasses. The observation that *Dpt* levels are low in CR^{Rel} and GF^{WT} animals, when compared to guts of CR^{WT} flies, indicates that basal *Dpt* expression in the gut is dependent on the presence of commensal microbiota.

In summary, our data indicate that commensal microbiota trigger ectopic activation of Imd signaling in *pims* loss-of-function mutants. Therefore, PIMS seems to act as a safety mechanism that protects the gut—and to a lesser extent—the fat body, from constitutive commensal microbiota-mediated and Imd-dependent activation of AMPs.

Loss of *pims* Results in Hyperactivation of the Imd Response Following Systemic Bacterial Infection

To investigate the function of *pims* in controlling the immune response following septic injury, we compared the Imd response of WT flies to the one of *pims* mutants. We found that *pims*-deficient individuals were not impaired in mounting an efficient immune response (data not shown). Using *Dpt* expression to measure the activity of the Imd pathway, we found that *E. coli* or *Ecc15*-stimulated *Dpt* expression in *pims* mutant animals was 2- to 3-fold above the levels of WT controls 2 hr, 8 hr, and

24 hr after a septic injury (Figures 3A and 3C). Interestingly, 8 hr after infection, *pims* seemed to be haploinsufficient since heterozygous mutant animals (*pims^{EY00723/+}*) also displayed elevated levels of *Dpt* expression (Figure 3A). Similar results were obtained using *pims* RNAi (Figure 3B). While the Imd response was significantly enhanced in *pims* mutants at 2 hr, 8 hr, and 24 hr, *Dpt* expression decreased at later time points and reached WT levels between 48 hr and 72 hr. This indicates that other negative regulators of Imd signaling operate normally in these animals. Loss of *pims* did not result in hyperactivation of the Toll pathway, as expression of *IM1* in *pims* mutants or *pims-IR* flies (Figures 3C and 3D) was not above the levels of WT animals challenged with the Gram-positive bacteria *Micrococcus luteus*. However, we noticed a moderate reduction (but no increase) in homozygous mutant animals. This indicates that PIMS selectively regulates Imd signaling. As *pims* expression is fully *Relish* dependent and acts to suppress Imd-mediated *Dpt* induction, *pims* appears to function in a negative-feedback loop that restricts Imd signaling.

pims Is Required to Limit the Immune Reaction in Response to Ingested Bacteria

In *Drosophila* adults, ingestion of nonpathogenic Gram-negative bacteria, such as *E. coli* and *Ecc15*, activates a strong local immune response in the gut (Zaidman-Rémy et al., 2006). However, these nonpathogenic bacteria do not trigger systemic activation of the immune response in the adult fat body (Zaidman-Rémy et al., 2006). This systemic immune tolerance to nonpathogenic Gram-negative bacteria relies, at least in part, on activation of the PGRP amidases PGRP-LB and PGRP-SC1/2 (Bischoff et al., 2006; Zaidman-Rémy et al., 2006). Imd-mediated activation of PGRP-LB and PGRP-SC results in the degradation of bacterial peptidoglycans; hence, it reduces the levels of the main elicitor required for the activation of a systemic immune reaction (Bischoff et al., 2006; Mellroth et al., 2003; Zaidman-Rémy et al., 2006).

To test the contribution of *pims* in establishing systemic immune tolerance to ingested Gram-negative bacteria, we fed *Ecc15*-contaminated food to WT and *pims* mutant flies. While WT flies did not mount an immune reaction, *pims* mutants and *pims-IR* flies significantly induced *Dpt* expression (Figures 4A and 4B), corresponding to about 10% of maximal levels of *Dpt* observed upon systemic infection by septic injury. Homozygous

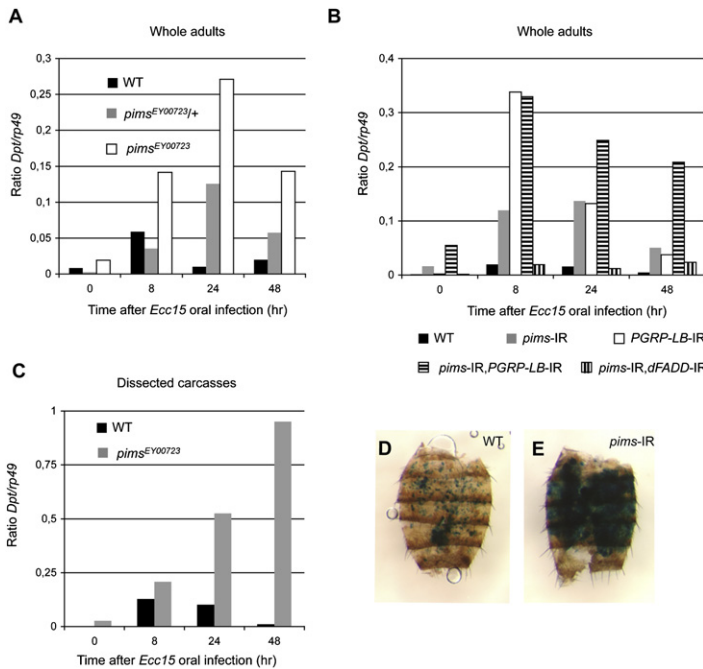


Figure 4. PIMS Is Required to Limit the Immune Reaction in Response to Ingested Bacteria

(A–C) Quantitative RT-qPCR analysis of *Diptericin* (*Dpt*) induction after *Ecc15* oral infection. *Dpt* expression is shown in *Canton*^S, *pims*^{EY00723/+} and *pims*^{EY00723} flies (A) and *Canton*^S and *pims*^{EY00723} carcasses (B). In (C), *Dpt* expression in *Da-GAL4/+*, *Da-GAL4 > pims-IR*, *Da-GAL4 > PGRP-LB-IR*, *Da-GAL4 > pims-IR,PGRP-LB-IR*, and *Da-GAL4 > pims-IR,dFADD-IR* flies is shown. *rp49* was used as the experimental expression standard.

(D and E) Activation of *Dpt-LacZ* in *pims*-IR carcasses upon *Ecc15* oral infection. In (C), representative X-gal staining of a *Dpt-LacZ*; *Da-GAL4/+* carcass (23.5%, *n* = 17) and a (D) *Dpt-LacZ*; *Da-GAL4 > pims-IR* carcass (34%, *n* = 35) 40 hr following *Ecc15* oral infection is shown.

pims mutant animals had a 27-fold increase in *Dpt* expression relative to WT controls. Interestingly, in this setting, *pims* was also haploinsufficient since heterozygous mutant animals (*pims*^{EY00723/+}) also displayed a 12.5-fold increase in *Dpt* expression (Figure 4A). Strikingly, this mimics the phenotype of *PGRP-LB* RNAi flies (Figure 4B) (Zaidman-Rémy et al., 2006). Of note, flies in which both *pims* and *dFADD* were depleted by RNAi had no such induction of *Dpt*, reinforcing the notion that *pims* functions genetically upstream of *dFADD* (Figure 4B). Finally, flies with coRNAi of *pims* and *PGRP-LB* showed a prolonged systemic response but unaltered intensity (Figure 4B).

To validate the systemic nature of the antimicrobial response, we analyzed *Dpt* expression in the fat body of WT and *pims*^{EY00723} mutant flies following ingestion of *Ecc15*. Strikingly, *pims* mutant animals that were fed on *Ecc15*-contaminated food had a dramatic increase in fat body-specific *Dpt* expression relative to WT controls (Figure 4C). We also analyzed expression of the *Dpt-LacZ* reporter in the fat body of WT and *pims*-IR flies orally infected with *Ecc15*. A 76.5% of WT flies (*n* = 17) failed to show any marked *Dpt-LacZ* expression, while some (23.5%) showed moderate, localized expression (Figure 4D). In contrast, 34% of *pims*-IR flies (*n* = 35) showed strong fat body-specific *Dpt-LacZ* activity, which is never seen in WT flies, and resembles levels observed upon septic injury (Figure 4E and data not shown). A further 26% of *pims* mutants showed a similar patchy staining pattern (Figure 4D), as seen in the 23.5% of WT flies (data not shown). Taken together, these data indicate that loss of *pims* function, like loss of *PGRP-SC1/2* and *PGRP-LB* (Bischoff et al., 2006; Zaidman-Rémy et al., 2006), disrupts systemic immune tolerance to ingested *Ecc15* bacteria.

PIMS Physically Associates with PGRP-LCx and Causes Its Depletion from the Plasma Membrane

To gain insight into the biochemical mechanism by which PIMS negatively regulates the Imd pathway, we tested the ability of

PIMS to bind to components of the Imd pathway. Interestingly, PIMS readily copurified PGRP-LCx from S2 cellular extracts (Figure 5A). However, under the same conditions, it did not interact with DIAP2, *dFADD*, and *Dredd* (data not shown). Reciprocal coimmunoprecipitation assays confirmed the interaction between PIMS and PGRP-LCx (Figure 5B). PIMS also interacted with a PGRP-LCx mutant that carries a point mutation in the RHIM (RIP homotypic interaction motif) domain required for activation of the Imd pathway (Kaneko et al., 2006) (data not shown). In addition to binding to PGRP-LCx, PIMS also bound to Imd, albeit significantly weaker (Figure 5C). The notion that PIMS associates, either directly or indirectly, with Imd is also supported by the observation that PIMS was independently identified in parallel experiments in which we performed large-scale affinity purification of Imd-associated protein complexes followed by mass-spectrometric analysis (data not shown). However, given the relatively weak association between Imd and PIMS, we anticipate that this interaction is indirect and most likely mediated by PGRP-LCx. Under the same conditions, PIMS failed to bind Wengen, a *Drosophila* member of the tumour necrosis factor receptor superfamily (Kanda et al., 2002) (Figure 5D). This indicates that PIMS specifically interacts with PGRP-LCx and is not a general receptor-interacting protein.

We noticed in our binding studies that coexpression of PIMS and PGRP-LCx resulted in depletion of PGRP-LCx protein levels. Consistently, expression of increasing amounts of PIMS resulted in the complete loss of PGRP-LCx (Figure 5E), while Wengen was not affected (data not shown). Under the same conditions, coexpression of Imd had no effect on the levels of PGRP-LCx (data not shown). Although we did not identify an obvious mammalian ortholog of PIMS, PIMS-mediated depletion of PGRP-LCx was also fully functional in mammalian HEK293T cells (Figure S2A). The observation that PIMS can deplete PGRP-LCx in insect and mammalian cells suggests that the machinery necessary for the removal of PGRP-LCx is evolutionarily conserved. Notably, PIMS harbors no recognizable domain that would be conserved at the level of primary amino acid sequence (data not shown).

Next, we tested whether PGRP-LCx depletion is due to degradation. However, treatment with proteasome or lysosome inhibitors did not affect PIMS-mediated reduction of PGRP-LCx (data not shown). Instead, coexpression of PIMS targeted PGRP-LCx to the Triton X-100-insoluble cell fraction (Figure 5F), which is

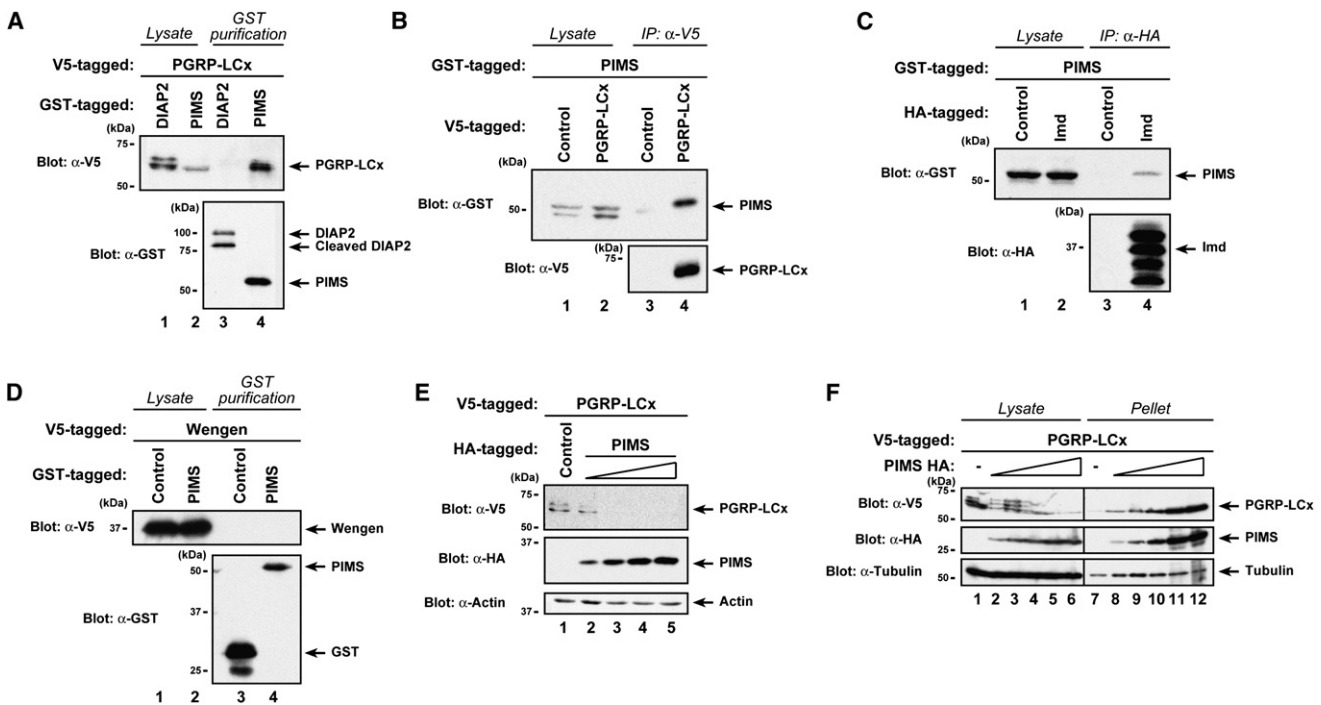


Figure 5. PIMS Interacts with PGRP-LCx

(A) Affinity purification of DIAP2-GST or PIMS-GST with V5-PGRP-LCx. Note that the PGRP-LCx-detected signals are reduced in the presence of PIMS.

(B) V5-PGRP-LCx was used to coimmunoprecipitate PIMS-GST from cellular extracts.

(C and D) Coaffinity purification of GST-PIMS with Imd-HA (C) or Wengen-V5 (D).

(E) PGRP-LCx protein levels are decreased by coexpression with increasing amounts of PIMS-HA.

(F) Coexpression of PIMS and PGRP-LCx leads to its accumulation in the Triton X-insoluble fraction. Lysate denotes Triton X-soluble fraction (lanes 1–6), whereas Pellet refers to Triton X-insoluble fraction (lanes 7–12). Tubulin was used as loading control.

consistent with PIMS changing the subcellular localization and surface availability of PGRP-LCx. Accordingly, coexpression of PIMS increased the amount of PGRP-LCx in the Triton X-100-insoluble fraction, while PGRP-LCx decreased in the detergent-soluble fraction.

Our above results indicate that PIMS acts as a negative regulator of PGRP-LCx. Given that *pims* loss-of-function mutants displayed enhanced induction of Imd signaling, we reasoned that ectopic expression of *pims* in S2 cells would block signaling through the Imd pathway. Consistently, expression of PIMS significantly reduced induction of *Drosocin*, another antimicrobial target gene of the Imd-signaling cascade, upon treatment with DAP-PGN or expression of PGRP-LCx (Figure 6A). In contrast, PIMS expression did not change *Drosocin* induction triggered by expression of a constitutively active form of *Relish* (data not shown). Coexpression of PIMS with PGRP-LCx also led to a significant reduction of PGRP-LCx protein levels (Figure 6A, lower panel). These results are consistent with the view that PIMS suppresses Imd signaling by downregulating PGRP-LCx levels.

Next, we examined the effects of PIMS on PGRP-LCx by confocal microscopy immunofluorescence. To this end, we used S2 cells and mammalian U2OS cells due to their “spreadout” morphology (Figures 6 and S2). As expected, PGRP-LCx, which is a transmembrane receptor in flies, was present in the plasma membrane, and to some extent, throughout the cytoplasm (Fig-

ures 6B and S2B). PIMS, on the other hand, appeared to be predominantly cytoplasmic (Figures 6C and S2C) and located partly in speckles. Importantly, coexpression of PIMS and PGRP-LCx caused a dramatic change in the subcellular localization of PGRP-LCx (Figures 6D and S2D). In the presence of PIMS, PGRP-LCx was no longer membrane localized and instead, was found in perinuclear structures, where it partially colocalized with PIMS. These results are consistent with the observed accumulation of PGRP-LCx in the Triton X-100-insoluble fraction and suggest that PIMS either triggers the internalization of PGRP-LCx or, alternatively, prevents PGRP-LCx from reaching the plasma membrane.

DISCUSSION

Drosophila innate immune responses rely on Toll and Imd signaling that activate transcriptional programs dedicated to kill infecting microbes (Ferrandon et al., 2007). In addition, such programs also induce modulators that through negative feedback regulate their temporal outputs to achieve balanced immune responses upon infection. Tight regulation is vital since misbalanced and prolonged responses are detrimental to the host (Bischoff et al., 2006; Ha et al., 2005a; Kim et al., 2007). Importantly, such immune modulators are also crucial during normal conditions, when the host is not exposed to invasive microbes. Under such conditions, inhibitors help to set up a buffered threshold

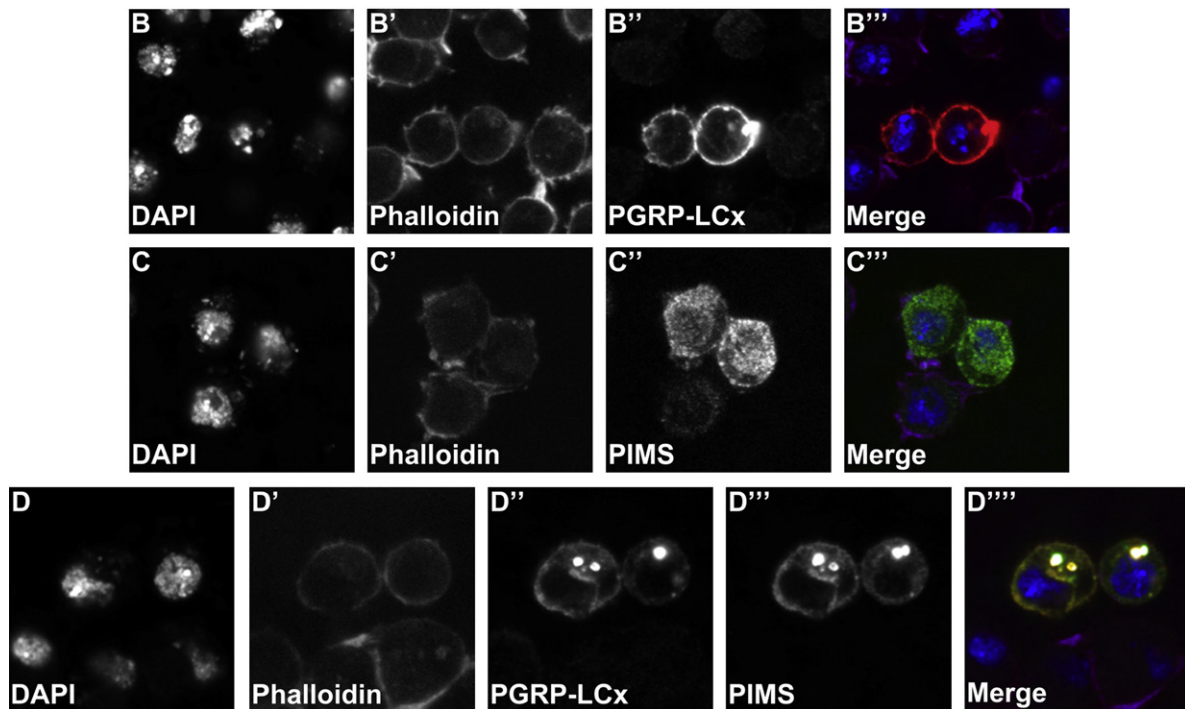
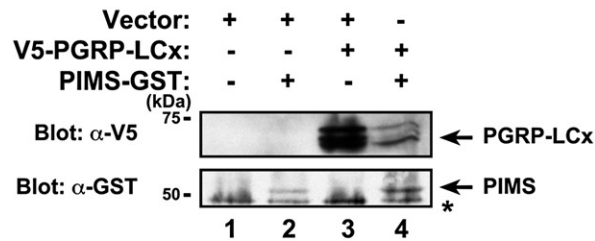
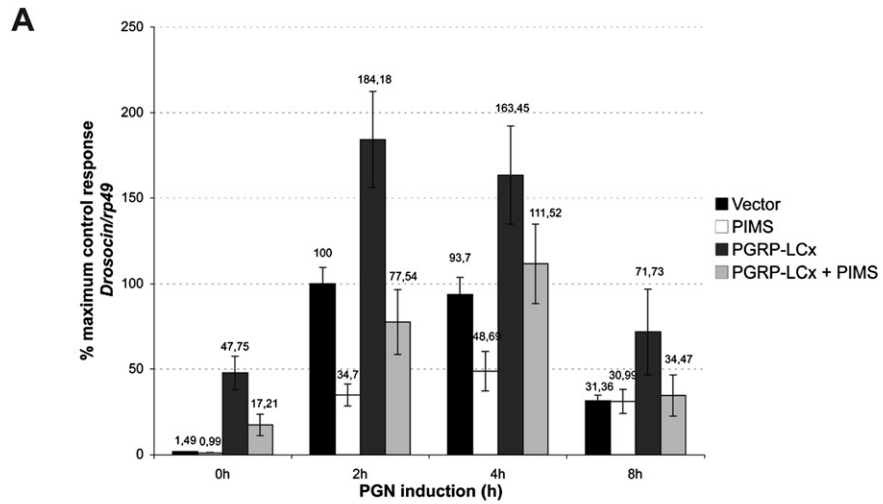


Figure 6. PIMS Inhibits Imd Signaling and Changes the Subcellular Localization of PGRP-LCx

(A) PIMS inhibits AMPs expression in S2 cells and downregulates PGRP-LCx protein. Time course of *Drosocin* expression in S2 cells transfected with vector control (black bars), PIMS (white bars), PGRP-LCx (dark gray bars), or PGRP-LCx and PIMS (light gray bars) is shown. The relative expression ratios of *Drosocin/rp49* are shown. Maximal *Drosocin* expression (2 hr) was set as 100%. Results are the average \pm SD of the relative expression ratios of *Drosocin/rp49* from at

required for immune tolerance and commensal host-microbe relationships (Maillet et al., 2008; Ryu et al., 2008; Zaidman-Rémy et al., 2006). Here, we demonstrate that PIMS is required to establish immune tolerance to commensal bacteria and to maintain a balanced Imd response following exposure to local bacterial infections. Consistent with a recent report (Kleino et al., 2008), we propose that PIMS/PIRK functions as a negative regulator of Imd signaling.

Several lines of evidence support the notion that PIMS functions as an immune modulator. First, disruption of *pims* causes loss of immune tolerance to nonpathogenic bacteria. Even in the absence of infection, *pims* mutant animals display expression of AMP genes in the gut, and to some extent in fat body cells, which is due to the presence of commensal bacteria in conventionally reared animals. Moreover, upon ingestion of nonpathogenic bacteria, which normally do not elicit a strong systemic immune response, individuals with depleted levels of *pims* significantly activate the Imd pathway in the fat body. Second, like the immune modulators *PGRP-LB* and *PGRP-SC1*, expression of *pims* is Relish dependent. Third, overexpression of PIMS suppresses AMP induction, while loss of *pims* results in their ectopic expression or hyperactivation, which is consistent with the notion that PIMS negatively regulates Imd-dependent immune responses. Fourth, PIMS interacts with *PGRP-LC*, the activating receptor of the Imd cascade, and likely downregulates *PGRP-LC* levels at the cell membrane. Finally, *pims* mutants phenocopy the systemic effects of the loss of *PGRP-LB* and *PGRP-SC1/2* following ingestion of nonpathogenic bacteria.

The observation that conventionally reared animals express *pims* in the gut, whereas germ-free animals do not, indicates that *pims* expression is induced by the presence of commensal microbiota. Thus, under normal conditions, low levels of PIMS in the gut prevents local antimicrobial responses to indigenous bacteria. In addition, PIMS prevents a systemic immune reaction in response to commensals. This notion is suggested by the observation that ectopic, fat body-specific expression of *Dpt* is abolished when *pims* mutant flies are reared under germ-free conditions. The relatively weak ectopic AMP expression of conventionally reared *pims* mutant flies may simply be due to the low levels of available peptidoglycans. Accordingly, higher levels of peptidoglycans, either by oral infection with nonpathogenic *Ecc15* or systemic bacterial infection, result in a dramatic activation of fat body-specific AMP expression. Taken together, our data are consistent with the view that PIMS contributes to the threshold of the Imd immune response, thereby establishing immune tolerance and development of host-commensal interactions.

PIMS also seems to be required for modulating the signal strength of the Imd pathway following infection. Consistently, *pims* is strongly induced in animals that face bacterial challenge. The intense and acute induction of *pims* suggests that high levels of PIMS are necessary to modulate Imd-mediated responses to

infection. Consistently, we find that *pims* is haploinsufficient in suppressing responses to local or systemic bacterial challenge.

Like PIMS, *PGRP-LB* and *PGRP-SC1/2* are similarly required to establish the threshold for the Imd immune response (Bischoff et al., 2006; Zaidman-Rémy et al., 2006). Since these PGRPs cleave DAP-PGN, they provide immune tolerance by degrading bacterial elicitors. Moreover, they also modulate the intensity of the immune response following bacterial infection and act as detoxifying enzymes (Bischoff et al., 2006; Zaidman-Rémy et al., 2006). Similar to *pims*, induced expression of *PGRP-LB* and *PGRP-SC1* are also under the control of Relish. Therefore, *PGRP-LB*, *PGRP-SC1*, and PIMS function in a negative-feedback response that enables immune modulation according to the severity of infection (Figure 7). In addition, *PGRP-LF*, *SCF^{Simb}*, and Caspar also negatively regulate Imd signaling. However, they seem to impinge on the pathway differently since mutation of *PGRP-LF*, *SCF^{Simb}*, and Caspar result in phenotypes that are distinct from those of *pims*, *PGRP-LB*, and *PGRP-SC1/2* mutant flies. Although, *PGRP-LF*, *SCF^{Simb}*, and Caspar mutants also show an increase in the basal activities of Imd signaling, their systemic response to micro-organisms is not significantly enhanced (Khush et al., 2002; Kim et al., 2006; Maillet et al., 2008).

Recent studies indicate that healthy flies harbor significant amounts of commensal bacteria (Cox and Gilmore, 2007; Ren et al., 2007; Ryu et al., 2008). However, little is known how the host tolerates them while mounting a full response to others. Our observations are consistent with a model in which *pims* acts as an immune modulator that, together with *PGRP-LB* and *PGRP-SC1/2*, establishes a buffered threshold for the activation of Imd-dependent AMP production. Such a threshold allows immune tolerance and the development of commensal host-bacteria interactions. Since *pims* expression is dependent on Relish, our data suggest that the Imd signal transduction pathway regulates its own inhibition through a negative-feedback mechanism that involves PIMS, *PGRP-LB*, and *PGRP-SC1* (Figure 7). While *PGRP-LB* and *PGRP-SC1* degrade the elicitor DAP-PGN, PIMS binds to *PGRP-LCx*, leading to its mislocalization. The concerted action of these immune modulators results in a self-regulating, buffered “oscillating cycle” of Imd-pathway activity. This would ensure low responsiveness to DAP-PGN of commensal bacteria. Given the conserved role of peptidoglycans as elicitors of immune responses (Chaput and Boneca, 2007) and in the establishment of beneficial reciprocal host-microbe interactions (Koropatnick et al., 2004; Ryu et al., 2008), this model may provide a blueprint for host-microbe interactions that is likely to be conserved in other metazoans, including vertebrates.

EXPERIMENTAL PROCEDURES

Fly Stocks

Canton^S and flies with one copy of *Daughterless-GAL4* (*da-GAL4*) were used as WT controls as appropriate. *Relish^{E20}*, *Dpt-LacZ*, and *da-GAL4* fly strains

least three independent experiments. The expression levels were assessed by immunoblot analysis with the indicated antibodies. An asterisk denotes a nonspecific band. The graph represents the mean \pm SD of *Drosocin/rp49* ratios from three independent experiments.

(B–D) Analysis of the subcellular localization of *PGRP-LCx* and PIMS in S2 cells. DAPI (blue, B''' and C''') was used as DNA label, and phalloidin (magenta, B''' and C''') was used as a marker for the actin cortex underneath the plasma membrane. Note the membrane localization of *PGRP-LCx* (red, B''' and C'''), while PIMS is predominantly cytoplasmic (green, C''' and D'''). Coexpression of PIMS and *PGRP-LCx* (D–D''') alters the subcellular localization of *PGRP-LCx*.

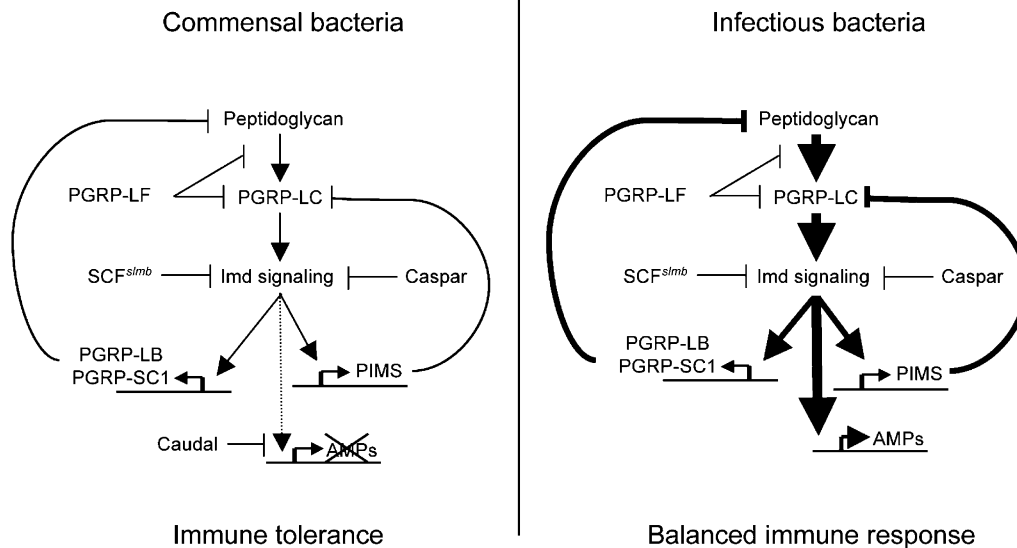


Figure 7. Model for the Regulation of Immune Reactions in Response to Commensal and Infectious Bacteria in *Drosophila*

pims functions as immune modulator, which together with *PGRP-LB* and *PGRP-SC1*, establishes a buffered threshold for Imd-dependent AMP production. Relish activates PIMS, PGRP-LB, and PGRP-SC1, which, in a negative-feedback loop, regulates Imd-signaling by relocating PGRP-LCx and degrading DAP-PGN, respectively. This results in a self-regulating state ensuring low responsiveness to DAP-PGN from commensal bacteria and allowing balanced immune responses following infections.

were described previously (Leulier et al., 2002). *Df(2R)ED3923*, *pims*^{EY00723}, UAS-*pims*-IR, UAS-*PGRP-LB*-IR, and UAS-*dFADD*-IR were obtained from the Bloomington *Drosophila* Stock Center, the Vienna *Drosophila* RNAi, or the National Institute of Genetics Stock Centers. Axenic *Canton^s* and *pims*^{EY00723} stocks were generated by bleaching and culturing embryos on autoclaved polenta-agar medium. Emerging flies were maintained on autoclaved standard medium. The presence of bacteria in fly homogenates was tested by PCR to detect 16S rRNA gene using eubacterial primers and by culturing the homogenates on Brain-Heart Infusion agar plates (Figure S1). Crosses were performed at 23°C apart from those with UAS-RNAi lines, which were started at 23°C until the L3 stage, and then transferred to 29°C.

Bacterial Strains and Infection Experiments

Septic injuries were performed by pricking adult males with a thin needle contaminated with *M. luteus* or *E. coli*. Adult oral infections were performed using female flies. Animals were previously starved for 2 hr at 29°C. Flies were fed on a 1.25% sucrose solution contaminated with concentrated *E. carotovora carotovora 15* (final optical density ~100) and incubated at 29°C.

Quantitative Real-Time PCR

Quantitative real-time PCR, TaqMan, and SYBR Green analysis were performed as previously described (Leulier et al., 2003). Primer information can be obtained upon request. The amount of mRNA detected was normalized to control *rp49* mRNA values. Normalized data was used to quantify the relative levels of a given mRNA according to cycling threshold analysis (ΔCt). For Figures 3 and 4, the $\Delta Ct^{Dpt \text{ or } IM1} / \Delta Ct^{rp49}$ ratios are indicated to allow comparison of the actual expression levels. For Figures 1 and 2, the relative $\Delta Ct^{Dpt \text{ or } pims} / \Delta Ct^{rp49}$ ratios of WT controls were set as 1, and the fold differences were indicated. For Figures 1A, 1B, 1G, 1H, 3, and 4, a pool of 20 flies were examined. One representative experiment is presented out of a minimum of three independent repeats. For Figures 1D, 1F, and 2G-I, graphs represent the mean and SD of relative ratios detected in three biological repetition of a pool of 20 flies, guts, and carcasses. For Figure 6A, the graph represents the mean and SD of *Drosocin/rp49* ratios from three independent experiments.

β -Galactosidase Staining

β -galactosidase staining was performed as previously described (Basset et al., 2000). Briefly, adult guts and carcasses were dissected in PBS, fixed for 5 min

in 0.5% glutaraldehyde on ice, washed in PBS, and incubated at 37°C in β -gal staining buffer for 3 hr (gut) or 16 hr (carcass).

Generation of Constructs and Antibodies

cDNA encoding the indicated proteins were cloned by PCR into pMTIZ-GST, pMT (Invitrogen), or pcDNA3. Constructs were verified by DNA sequencing. Point mutants were generated by site-directed mutagenesis (Stratagene), according to the manufacturer's instructions. α -V5 (Serotec), α -GST (GE Healthcare), α -actin (Santa Cruz Biotechnology), α -HA (Roche Diagnostics), α -FLAG (SIGMA), α -tubulin (SIGMA), Alexa633-conjugated α -phalloidin (Invitrogen), α -Myc (Santa Cruz Biotechnology), and Alexa488- and Alexa555-conjugated secondary antibodies (Alexa) were used according to the manufacturer's instructions.

Tissue Culture and Induction of Imd Response

Cells were cultured as described previously (Leulier et al., 2006) and transfected with either calcium phosphate (BD Biosciences), Effectene (QIAGEN), or FuGENE 6 (Roche Diagnostics). For induction of Imd signaling in S2 cells, cells were treated with 10 μ g/ml of commercially available LPS (SIGMA) for the indicated time intervals. Please note that commercially available LPS contains PGN, which induces expression of AMPs (Leulier et al., 2003).

Immunoprecipitation and Immunoblot Analysis

Immunoprecipitation assays were performed as described previously (Leulier et al., 2006). Glutathione-sepharose 4B beads (Amersham Biosciences), monoclonal α -HA-coupled agarose beads (HA-7 clone, SIGMA), and α -V5-coupled agarose gel (V5-10 clone, SIGMA) were used to purify tagged proteins. Samples were separated by SDS-PAGE and examined by immunoblot analysis using either chemiluminescence (Amersham Biosciences) or Odyssey Technology (LI-COR Biosciences).

Confocal Microscopy and Image Acquisition

Confocal microscopy was performed as previously described (Tenev et al., 2002). All pictures were processed using Adobe Photoshop CS2 software.

SUPPLEMENTAL DATA

Supplemental Data include two figures and can be found online at <http://www.cellhostandmicrobe.com/cgi/content/full/4/2/147/DC1/>.

ACKNOWLEDGMENTS

We thank Neal Silverman for sharing unpublished data, Isabelle Vallet-Gely for critical reading of the manuscript, the Bloomington Stock Center, the Vienna *Drosophila* RNAi Center, and the National Institute of Genetics Fly Stock Center for fly lines. P.S.R. is supported by a fellowship (SFRH/BD/15219/2004) from the Fundação para a Ciência e Tecnologia in Portugal. F.L. was partly funded by a long-term HFSP Fellowship. This work was supported by ANR-05-MIIM-016-01 and by the Bettencourt-Schueller Foundation.

Received: April 28, 2008

Revised: June 19, 2008

Accepted: July 16, 2008

Published: August 13, 2008

REFERENCES

- Artis, D. (2008). Epithelial-cell recognition of commensal bacteria and maintenance of immune homeostasis in the gut. *Nat. Rev. Immunol.* 8, 411–420.
- Backhed, F., Ley, R.E., Sonnenburg, J.L., Peterson, D.A., and Gordon, J.I. (2005). Host-bacterial mutualism in the human intestine. *Science* 307, 1915–1920.
- Basset, A., Khush, R., Braun, A., Gardan, L., Boccard, F., Hoffmann, J., and Lemaitre, B. (2000). The phytopathogenic bacteria, *Erwinia carotovora*, infects *Drosophila* and activates an immune response. *Proc. Natl. Acad. Sci. USA* 97, 3376–3381.
- Bischoff, V., Vignal, C., Duvic, B., Boneca, I.G., Hoffmann, J.A., and Royet, J. (2006). Downregulation of the *Drosophila* immune response by peptidoglycan-recognition proteins SC1 and SC2. *PLoS Pathog.* 2, e14.
- Busse, M.S., Arnold, C.P., Towb, P., Katrivesis, J., and Wasserman, S.A. (2007). A kappaB sequence code for pathway-specific innate immune responses. *EMBO J.* 26, 3826–3835.
- Casadevall, A., and Pirofski, L.A. (2000). Host-pathogen interactions: basic concepts of microbial commensalism, colonization, infection, and disease. *Infect. Immun.* 68, 6511–6518.
- Chaput, C., and Boneca, I.G. (2007). Peptidoglycan detection by mammals and flies. *Microbes Infect.* 9, 637–647.
- Chintapalli, V.R., Wang, J., and Dow, J.A. (2007). Using FlyAtlas to identify better *Drosophila melanogaster* models of human disease. *Nat. Genet.* 39, 715–720.
- Choe, K.M., Werner, T., Stoven, S., Hultmark, D., and Anderson, K.V. (2002). Requirement for a peptidoglycan recognition protein (PGRP) in Relish activation and antibacterial immune responses in *Drosophila*. *Science* 296, 359–362.
- Cox, C.R., and Gilmore, M.S. (2007). Native microbial colonization of *Drosophila melanogaster* and its use as a model of *Enterococcus faecalis* pathogenesis. *Infect. Immun.* 75, 1565–1576.
- De Gregorio, E., Spellman, P.T., Tzou, P., Rubin, G.M., and Lemaitre, B. (2002). The Toll and Imd pathways are the major regulators of the immune response in *Drosophila*. *EMBO J.* 21, 2568–2579.
- Ferrandon, D., Jung, A.C., Crique, M., Lemaitre, B., Uttenweiler-Joseph, S., Michaut, L., Reichhart, J., and Hoffmann, J.A. (1998). A drosomycin-GFP reporter transgene reveals a local immune response in *Drosophila* that is not dependent on the Toll pathway. *EMBO J.* 17, 1217–1227.
- Ferrandon, D., Imler, J.L., Hetru, C., and Hoffmann, J.A. (2007). The *Drosophila* systemic immune response: sensing and signalling during bacterial and fungal infections. *Nat. Rev. Immunol.* 7, 862–874.
- Foley, E., and O'Farrell, P.H. (2004). Functional dissection of an innate immune response by a genome-wide RNAi screen. *PLoS Biol.* 2, E203.
- Gottar, M., Gobert, V., Michel, T., Belvin, M., Duyk, G., Hoffmann, J.A., Ferrandon, D., and Royet, J. (2002). The *Drosophila* immune response against Gram-negative bacteria is mediated by a peptidoglycan recognition protein. *Nature* 416, 640–644.
- Ha, E.M., Oh, C.T., Bae, Y.S., and Lee, W.J. (2005a). A direct role for dual oxidase in *Drosophila* gut immunity. *Science* 310, 847–850.
- Ha, E.M., Oh, C.T., Ryu, J.H., Bae, Y.S., Kang, S.W., Jang, I.H., Brey, P.T., and Lee, W.J. (2005b). An antioxidant system required for host protection against gut infection in *Drosophila*. *Dev. Cell* 8, 125–132.
- Kallio, J., Leinonen, A., Ulvila, J., Valanne, S., Ezekowitz, R.A., and Ramet, M. (2005). Functional analysis of immune response genes in *Drosophila* identifies JNK pathway as a regulator of antimicrobial peptide gene expression in S2 cells. *Microbes Infect.* 7, 811–819.
- Kanda, H., Igaki, T., Kanuka, H., Yagi, T., and Miura, M. (2002). Wengen, a member of the *Drosophila* tumor necrosis factor receptor superfamily, is required for Eiger signaling. *J. Biol. Chem.* 277, 28372–28375.
- Kaneko, T., Yano, T., Aggarwal, K., Lim, J.H., Ueda, K., Oshima, Y., Peach, C., Erturk-Hasdemir, D., Goldman, W.E., Oh, B.H., et al. (2006). PGRP-LC and PGRP-LE have essential yet distinct functions in the *Drosophila* immune response to monomeric DAP-type peptidoglycan. *Nat. Immunol.* 7, 715–723.
- Khush, R.S., Cornwell, W.D., Uram, J.N., and Lemaitre, B. (2002). A ubiquitin-proteasome pathway represses the *Drosophila* immune deficiency signaling cascade. *Curr. Biol.* 12, 1728–1737.
- Kim, M., Lee, J.H., Lee, S.Y., Kim, E., and Chung, J. (2006). Caspar, a suppressor of antibacterial immunity in *Drosophila*. *Proc. Natl. Acad. Sci. USA* 103, 16358–16363.
- Kim, L.K., Choi, U.Y., Cho, H.S., Lee, J.S., Lee, W.B., Kim, J., Jeong, K., Shim, J., Kim-Ha, J., and Kim, Y.J. (2007). Down-regulation of NF-kappaB target genes by the AP-1 and STAT complex during the innate immune response in *Drosophila*. *PLoS Biol.* 5, e238.
- Kleino, A., Myllymaki, H., Kallio, J., Vanha-aho, L.M., Oksanen, K., Ulvila, J., Hultmark, D., Valanne, S., and Ramet, M. (2008). Pirk is a negative regulator of the *Drosophila* Imd pathway. *J. Immunol.* 180, 5413–5422.
- Koropatnick, T.A., Engle, J.T., Apicella, M.A., Stabb, E.V., Goldman, W.E., and McFall-Ngai, M.J. (2004). Microbial factor-mediated development in a host-bacterial mutualism. *Science* 306, 1186–1188.
- Lemaitre, B., and Hoffmann, J. (2007). The host defense of *Drosophila melanogaster*. *Annu. Rev. Immunol.* 25, 697–743.
- Leulier, F., Vidal, S., Saigo, K., Ueda, R., and Lemaitre, B. (2002). Inducible expression of double-stranded RNA reveals a role for dFADD in the regulation of the antibacterial response in *Drosophila* adults. *Curr. Biol.* 12, 996–1000.
- Leulier, F., Parquet, C., Pili-Floury, S., Ryu, J.H., Caroff, M., Lee, W.J., Mengin-Lecreux, D., and Lemaitre, B. (2003). The *Drosophila* immune system detects bacteria through specific peptidoglycan recognition. *Nat. Immunol.* 4, 478–484.
- Leulier, F., Ribeiro, P.S., Palmer, E., Tenev, T., Takahashi, K., Robertson, D., Zachariou, A., Pichaud, F., Ueda, R., and Meier, P. (2006). Systematic in vivo RNAi analysis of putative components of the *Drosophila* cell death machinery. *Cell Death Differ.* 13, 1663–1674.
- Liehl, P., Blight, M., Vodovar, N., Boccard, F., and Lemaitre, B. (2006). Prevalence of local immune response against oral infection in a *Drosophila*/Pseudomonas infection model. *PLoS Pathog.* 2, e56.
- Macdonald, T.T., and Monteleone, G. (2005). Immunity, inflammation, and allergy in the gut. *Science* 307, 1920–1925.
- Maillet, F., Bischoff, V., Vignal, C., Hoffmann, J., and Royet, J. (2008). The *Drosophila* peptidoglycan recognition protein PGRP-LF blocks PGRP-LC and IMD/JNK pathway activation. *Cell Host Microbe* 3, 293–303.
- Meister, M., Braun, A., Kappler, C., Reichhart, J.M., and Hoffmann, J.A. (1994). Insect immunity. A transgenic analysis in *Drosophila* defines several functional domains in the dipterin promoter. *EMBO J.* 13, 5958–5966.
- Mellroth, P., Karlsson, J., and Steiner, H. (2003). A scavenger function for a *Drosophila* peptidoglycan recognition protein. *J. Biol. Chem.* 278, 7059–7064.
- Müller, C.A., Autenrieth, I.B., and Peschel, A. (2005). Innate defenses of the intestinal epithelial barrier. *Cell. Mol. Life Sci.* 62, 1297–1307.
- Nehme, N.T., Liégeois-Liégeois, S., Kele, B., Giammarinaro, P., Pradel, E., Hoffmann, J.A., Ewbank, J.J., and Ferrandon, D. (2007). A model of bacterial intestinal infections in *Drosophila melanogaster*. *PLoS Pathog.* 3, e173.
- Önfelt Tingvall, T., Roos, E., and Engstrom, Y. (2001). The imd gene is required for local Cecropin expression in *Drosophila* barrier epithelia. *EMBO Rep.* 2, 239–243.

- Ren, C., Webster, P., Finkel, S.E., and Tower, J. (2007). Increased internal and external bacterial load during *Drosophila* aging without life-span trade-off. *Cell Metab.* *6*, 144–152.
- Ryu, J.H., Ha, E.M., Oh, C.T., Seol, J.H., Brey, P.T., Jin, I., Lee, D.G., Kim, J., Lee, D., and Lee, W.J. (2006). An essential complementary role of NF- κ B pathway to microbicidal oxidants in *Drosophila* gut immunity. *EMBO J.* *25*, 3693–3701.
- Ryu, J.H., Kim, S.H., Lee, H.Y., Bai, J.Y., Nam, Y.D., Bae, J.W., Lee, D.G., Shin, S.C., Ha, E.M., and Lee, W.J. (2008). Innate immune homeostasis by the homeobox gene *caudal* and commensal-gut mutualism in *Drosophila*. *Science* *319*, 777–782.
- Silverman, N., Zhou, J., Stööven, S., Pandey, N., Hultmark, D., and Maniatis, T. (2000). A *Drosophila* I κ B kinase complex required for Relish cleavage and antibacterial immunity. *Genes Dev.* *14*, 2461–2471.
- Stöven, S., Silverman, N., Junell, A., Hedengren-Olcott, M., Erturk, D., Engstrom, Y., Maniatis, T., and Hultmark, D. (2003). Caspase-mediated processing of the *Drosophila* NF- κ B factor Relish. *Proc. Natl. Acad. Sci. USA* *100*, 5991–5996.
- Stuart, L.M., and Ezekowitz, R.A. (2008). Phagocytosis and comparative innate immunity: learning on the fly. *Nat. Rev. Immunol.* *8*, 131–141.
- Takehana, A., Yano, T., Mita, S., Kotani, A., Oshima, Y., and Kurata, S. (2004). Peptidoglycan recognition protein (PGRP)-LE and PGRP-LC act synergistically in *Drosophila* immunity. *EMBO J.* *23*, 4690–4700.
- Tenev, T., Zachariou, A., Wilson, R., Paul, A., and Meier, P. (2002). Jafrac2 is an IAP antagonist that promotes cell death by liberating Dronc from DIAP1. *EMBO J.* *21*, 5118–5129.
- Tzou, P., Ohresser, S., Ferrandon, D., Capovilla, M., Reichhart, J.M., Lemaitre, B., Hoffmann, J.A., and Imler, J.L. (2000). Tissue-specific inducible expression of antimicrobial peptide genes in *Drosophila* surface epithelia. *Immunity* *13*, 737–748.
- Zaidman-Rémy, A., Hervé, M., Poidevin, M., Pili-Floury, S., Kim, M.S., Blanot, D., Oh, B.H., Ueda, R., Mengin-Lecreulx, D., and Lemaitre, B. (2006). The *Drosophila* amidase PGRP-LB modulates the immune response to bacterial infection. *Immunity* *24*, 463–473.